Neurosci. Bull. May, 2022, 38(5):548–552
https://doi.org/10.1007/s12264-022-00819-8

www.neurosci.cn
www.springer.com/12264

LETTER TO THE EDITOR

Optimal Timing of a Commonly-Used Rabies Virus for Neural Recording and Manipulation

Jing Chen[1] · Chunli Li[2] · Zhonghua Lu[4] · Cheng Zhan[2,3,5]

Received: 4 August 2021 / Accepted: 1 November 2021 / Published online: 29 January 2022

Dear Editor,

A fundamental goal of modern neuroscience is to dissect the neural circuits in the brain and understand their functions. As a powerful tool for anatomical studies, the genetically modified rabies virus (RV) SADΔG (EnvA) has achieved great success in mapping presynaptic inputs to genetically marked neurons [1–3]. In combination with chemogenetics, optogenetics, and Ca^{2+} indicators, many RV variants have been developed to manipulate and record activity in defined neural circuits [4]. However, RV infection greatly impacts cell survival [5], and several labs have made efforts to reduce its neurotoxicity [6–8]. Concerns about the neurotoxicity of RV and uncertainty about the viability of RV-infected neurons have largely limited the wider use of RV tools in physiological and behavioral experiments.

Even so, RV tools have been successfully applied in studies of neural circuit function [9–12]. The timing of neural recording and manipulation is the key to success in RV-based functional studies. It is important to record and manipulate RV-infected neurons before RV-induced toxicity causes severe damage to neurons. However, while it is known that most infected neurons are ablated within weeks, longitudinal investigations of the effects of RV infection on cell death and viability are scarce, which makes it challenging to choose the optimal timing to manipulate or record from infected neurons.

Here, we focus on a recently-identified gut-brain orexigenic neural circuit [13], in which catecholaminergic neurons in the nucleus of the solitary tract (NTS) receive direct inputs from vagal sensory neurons in the nodose ganglion (NG). We examined the effects of RV-induced toxicity on apoptosis and viability in NG neurons at different times after RV infection and then defined a feasible time window for applying SADΔG (EnvA) in functional studies of the NG→NTS circuit.

To characterize the neurotoxicity of the genetically modified RV SADΔG (EnvA), we used the Cre/LoxP gene-expression system to label presynaptic inputs to NTS catecholaminergic (CA^{NTS}) neurons (Fig. S1A, B). Briefly, two Cre-dependent AAV helper vectors, AAV-DIO-TVA-mCherry and AAV-DIO-RG, were injected into the NTS of *Dbh-Cre* mice, where Cre expression is under the control of the *dopamine-β-hydroxylase (Dbh)* promoter, which is a rate-limiting enzyme for the biosynthesis of catecholamines. Two weeks later, the SAD-ΔG-GFP(EnVA)

Supplementary Information The online version contains supplementary material available at https://doi.org/10.1007/s12264-022-00819-8.

Jing Chen and Chunli Li have contributed equally to this work.

✉ Cheng Zhan
zhancheng@ustc.edu.cn

[1] School of Sport Science, Beijing Sport University, Beijing 100084, China

[2] National Institute of Biological Sciences, Beijing 102206, China

[3] Department of Hematology, The First Affiliated Hospital of USTC, School of Life Sciences, Division of Life Sciences and Medicine, University of Science and Technology of China, Hefei 230026, China

[4] Shenzhen Key Laboratory for Molecular Biology of Neural Development, The Brain Cognition and Brain Disease Institute, Shenzhen Institute of Advanced Technology, Chinese Academy of Sciences, Shenzhen-Hong Kong Institute of Brain Science, Shenzhen 518055, China

[5] Tsinghua Institute of Multidisciplinary Biomedical Research, Tsinghua University, Beijing 100084, China

was injected into the same area of *Dbh-Cre* mice. The EnVA targets RV to specific neurons that express the cognate TVA viral receptor, and only when RG is expressed does the infection spread trans-synaptically. Using this strategy, we successfully labeled presynaptic inputs to CA^{NTS} neurons in several brain areas: the hypothalamic paraventricular nucleus (PVN), the parasubthalamic nucleus (PBN), the bed nucleus of the stria terminalis (BNST), and the basolateral amygdala (BLA) (Fig. S1C). Moreover, we observed many trans-synaptically-infected neurons in the NG (Fig. S1D).

We then assessed the neurotoxicity of SAD-ΔG-GFP(EnvA) in trans-synaptically-infected NG neurons. After RV injection into the NTS, NGs were collected on days 4, 7, 10, 14, and 18, and then subjected to a terminal deoxynucleotidyl transferase-mediated dUTP nick-end labeling (TUNEL) assay to assess apoptosis. On day 4 after RV injection, the numbers of apoptotic cells in the RV-infected NGs were slightly increased compared to those in negative control NGs, but the difference did not reach significance (Fig. S2A1, A3). From day 7 to day 18, RV infection induced much more severe apoptosis in the NG (Fig. S2A1, A3). In wild-type mice, many apoptotic cells were observed in DNase-treated NGs (as a positive control), whereas only few apoptotic cells were detected in phosphate-buffered saline-treated NGs (as a negative control) (Fig. S2A2, A3). Consistent with the trend for apoptosis, there were a number of RV-labeled NG neurons on days 4 and 7 after RV injection, but they rapidly decreased from day 10 to day 18 (Fig. S2A1, A4). To determine whether the decreased number of labeled NG neurons was due to increased apoptosis or just the termination of expression of the fluorescent marker gene in the RV genome, SAD-ΔG-Cre-GFP(EnvA) was injected into the NTS of *Net-Cre:Ai14* reporter mice (Fig. S2B1), in which expression of tdTomato fluorescence is permanent following *Cre*-mediated recombination. About 85% of tdTomato+ NG neurons were co-localized with GFP+ neurons on day 18 after RV infection (Fig. S2B2), suggesting that expression of RV-delivered GFP in RV-labeled neurons had not terminated. Thus, the disappearance of neurons from the NG was most likely due to increased apoptosis. These results suggested that: (1) RV infection causes severe apoptosis in NG neurons from day 7 post-infection, and (2) most infected NG neurons are ablated within ~18 days.

Next, to assess the viability of RV-infected NG neurons, a Cre-dependent AAV vector encoding the red fluorescent Ca^{2+} indicator jRGECO1a (AAV-DIO-jRGECO1a) was injected into the NG of *Dbh-Cre* mice. Since there is no Cre expression in the NG neurons of *Dbh-Cre* mice, SAD-ΔG-Cre-GFP(EnvA) was used to selectively express Cre in CA^{NTS}-projecting NG neurons (Fig. S3A, B). Ten days after RV injection, ~70% of $jRGECO1a^{+}$ NG neurons co-expressed GFP, suggesting highly selective expression of jRGECO1a in RV-infected NG neurons (GFP^{+}) (Fig. S3C).

We then applied in-vitro Ca^{2+} imaging to determine the activity of the RV-infected NG neurons. Four days after RV injection, perfusion of 60 mmol/L KCl but not Ringer's solution induced intense Ca^{2+} flux in RV-infected NG neurons (Fig. 1A1, A2 and Supplementary Movie 1). As a no-RV control, AAV-DIO-jRGECO1a was injected into the NG of *Glp1r-Cre* mice, in which glucagon-like peptide 1 receptor (GLP1R) neurons express Cre. As expected, 60 mmol/L KCl but not Ringer's solution induced intense Ca^{2+} flux in ~90% of the jRGECO1a+ NG neurons of *Glp1r-Cre* mice (Fig. 1A3, A4, and Supplementary Movie 2). Within one week after RV injection, the responsiveness of RV-infected NG neurons was comparable with that of no-RV controls, although there was a downward trend from day 4 to day 7 (Figs. 1B1, B2, S4A1 and A2, Supplementary Movie 3, and Table S1). These results suggested that NG neurons trans-synaptically infected with RV retain good viability within one week after RV injection.

Notably, from day 10 to day 18 after RV injection, both the percentage of cells that respond to KCl stimulation and the ΔF/F values of fluorescent Ca^{2+} signals in RV-infected NGs were less than that in the control group (Figs. 1B1, B2, S4, Supplementary Movies 4 and 5, and Table S1). Consistent with the apoptosis results, none of the $jRGECO1a^{+}$ NG neurons responded to 60 mmol/L KCl stimulation on day 18 after RV injection (Fig. 1B1, B2 and Table S1). These results suggested that the viability of RV-infected NG neurons declines quickly during this period.

Based on the above apoptosis and Ca^{2+} imaging results, we reasoned that an appropriate time window of RV-based neural manipulation was around one week after RV injection. We then applied RV-based chemogenetics to manipulate the NG→NTS neural circuit in freely-behaving mice. Using a strategy similar to expressing jRGECO1a in CA^{NTS}-projecting NG neurons, an excitatory chemogenetic vector hM3Dq was selectively expressed in the NG of *Npy-Cre* mice (Fig. 2A1). Seven days after RV injection, mice received an intraperitoneal injection of the hM3Dq ligand CNO (2 mg/kg). Administration of CNO induced many more Fos^{+} neurons in the NTS compared to saline injection (total 808 Fos+ neurons, 20.7 ± 2.1 per slice in the CNO group *versus* total 144 Fos+ neurons, 3.7 ± 0.4 per slice in the saline group, $P < 0.0001$; 39 brain slices from 3 mice in each group) (Fig. 2A2). Moreover, CNO administration induced Fos expression in ~20% of NTS starter neurons (1691 starter neurons in 39 brain slices from 3 mice), while very few starter neurons were activated in the saline-treated group (1444 starter neurons in 39 brain slices from 3 mice) (Fig. 2A3). These results showed that the NG→NTS neural

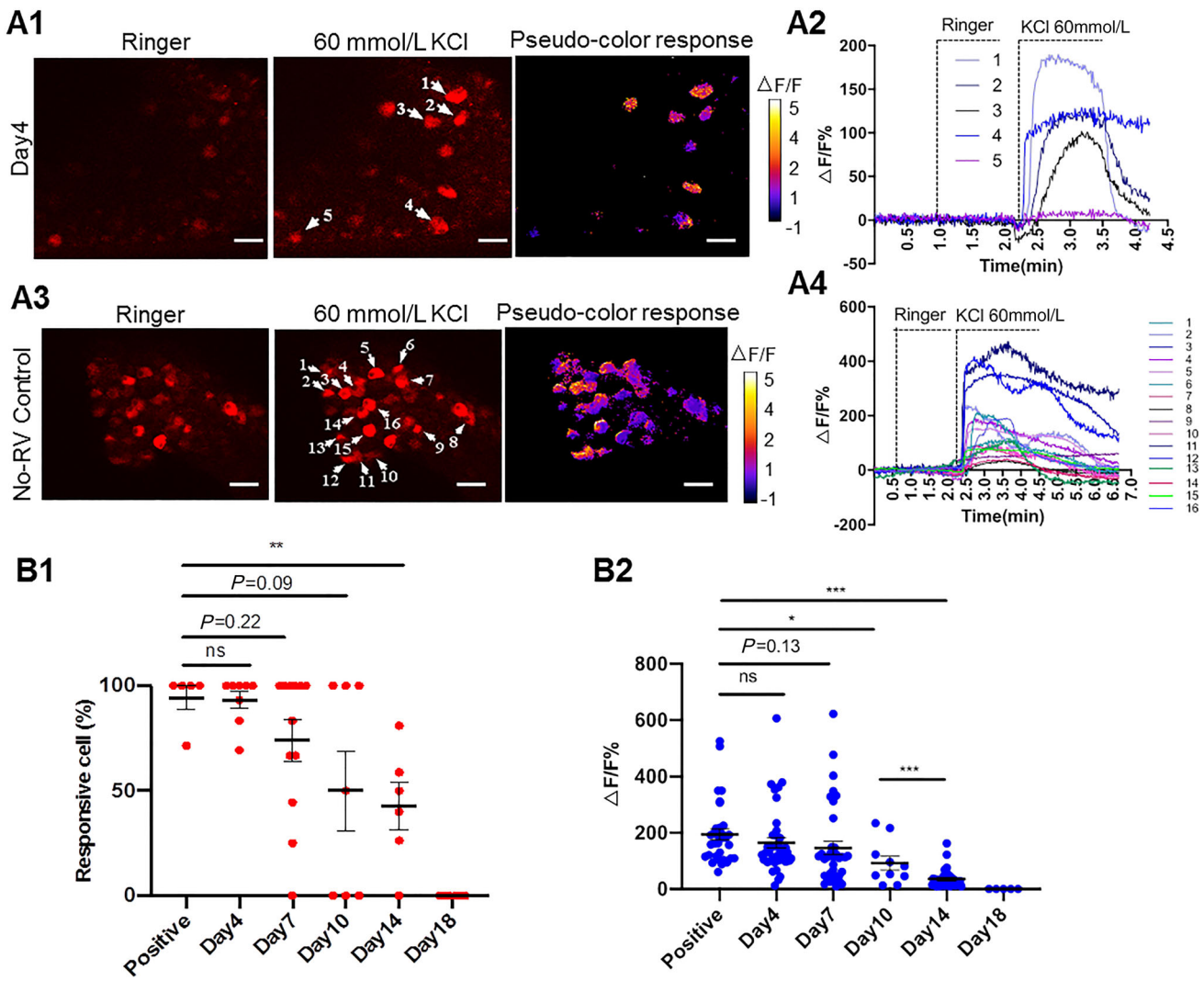

Fig. 1 Viability of RV-infected NG neurons. **A1**, **A2** Representative images and traces showing fluorescence responses to perfusion with Ringer's solution and 60 mmol/L KCl in JRGECO1a-expressing NG neurons on day 4 after RV infection. **A1** Representative images and corresponding fluorescence changes after RV injection (scale bars here and below, 50 μm). **A2** Traces of florescence changes in NG neurons in indicated neurons in **A1**. **A3**, **A4** Following injection of AAV-DIO-JRGECO1a into the NG of *Glp1r-Cre* mice, JRGECO1a is expressed in NG neurons as a no-RV control. **A3** Representative images and corresponding fluorescence changes in no-RV NG neurons in response to perfusion with Ringer's and 60 mmol/L KCl. **A4** Traces of fluorescence responses measured in indicated neurons in A3. **B1** Percentages of JRGECO1a$^+$ neurons that respond to KCl stimulation. Each symbol represents an imaging field of the NG. **B2** Peak fluorescence changes induced by KCl stimulation. Each symbol represents one neuron. mean ± s.e.m.; $^*P$ <0.05, $^{**}P$ <0.01, $^{***}P$ <0.001, Student's *t*-test.

circuit was chemogenetically activated *in vivo* on day 7 after RV infection.

We then applied the RV-based chemogenetic approach to examine the effect of activation of CA^{NTS}-projecting NG neurons on feeding behavior (Fig. 2B1). Following injection of SAD-ΔG-Cre-GFP(EnvA) into the NTS, hM3Dq was expressed in RV trans-synaptic-infected NG neurons (referred to as NG^{hM3Dq} mice) (Fig. 2B2). Mice receiving sham surgery were used as negative control. Seven to ten days after RV injection, administration of CNO (2 mg/kg, IP) but not saline significantly increased food intake in NG^{hM3Dq} mice (Fig. 2B3). CNO administration in control mice did not increase food intake, indicating that this effect was not due to any off-target effects of CNO (Fig. 2B3). These results suggested that activation of the NG→CA^{NTS} neural circuit successfully drove feeding behavior on days 7–10 after RV infection.

Given that the neurotoxicity of RV increases with prolonged infection, the timing of neuronal recording and manipulation is critical in RV-based functional studies. Here, we systematically and comprehensively characterized apoptosis and cell viability at different times after RV

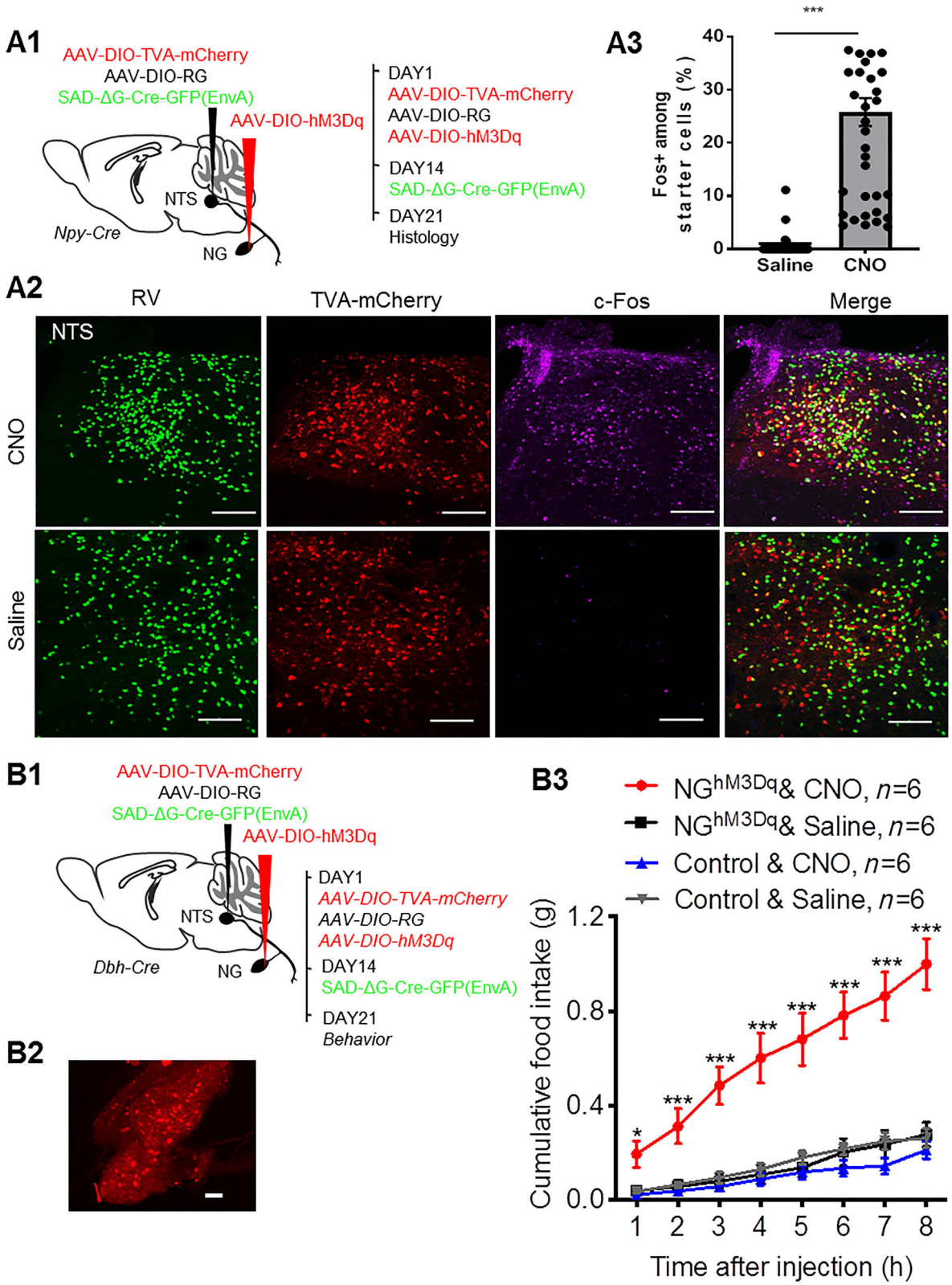
A1
AAV-DIO-TVA-mCherry
AAV-DIO-RG
SAD-ΔG-Cre-GFP(EnvA)
AAV-DIO-hM3Dq
NTS
Npy-Cre
NG
DAY1
AAV-DIO-TVA-mCherry
AAV-DIO-RG
AAV-DIO-hM3Dq
DAY14
SAD-ΔG-Cre-GFP(EnvA)
DAY21
Histology
A3
***
Fos+ among starter cells (%)
40
30
20
10
0
Saline
CNO
A2
RV
TVA-mCherry
c-Fos
Merge
NTS
CNO
Saline
B1
AAV-DIO-TVA-mCherry
AAV-DIO-RG
SAD-ΔG-Cre-GFP(EnvA)
AAV-DIO-hM3Dq
NTS
Dbh-Cre
NG
DAY1
AAV-DIO-TVA-mCherry
AAV-DIO-RG
AAV-DIO-hM3Dq
DAY14
SAD-ΔG-Cre-GFP(EnvA)
DAY21
Behavior
B2
B3
NGhM3Dq& CNO, n=6
NGhM3Dq& Saline, n=6
Control & CNO, n=6
Control & Saline, n=6
Cumulative food intake (g)
1.2
0.8
0.4
0.0
1 2 3 4 5 6 7 8
Time after injection (h)

◀**Fig. 2** Chemogenetic activation of CA^{NTS}-projecting NG neurons stimulated feeding. **A1–A3** RV-based chemogenetic activation-induced Fos signals in NTS starter cells. **A1** Experimental strategy of selective expression of hM3Dq in NPY^{NTS}-projecting NG neurons. **A2** Representative images showing co-localization of Fos^+ (purple) and RV^+TVA^+ (green and red) NTS starter neurons following CNO (upper panels) or saline (lower panels) administration. Scale bars, 100 μm. **A3** Percentages of Fos^+ neurons among NTS starter neurons. Each symbol represents a brain slice. Mean ± s.e.m.; Student's *t*-test. **B1–B3** Chemogenetic activation of CA^{NTS}-projecting NG neurons stimulates feeding. **B1** Experimental strategy of selective expression of hM3Dq in CA^{NTS}-projecting NG neurons. **B2** hM3Dq expression in NG neurons. Scale bar, 100 μm. **B3** Food intake in NG^{hM3Dq} and control mice following CNO or saline administration. $^*P < 0.05$, $^{**}P < 0.01$, $^{***}P < 0.001$, two-way ANOVA, CNO *vs* saline treatment in NG^{hM3Dq} mice.

infection, and revealed that trans-synaptically infected NG neurons retained good viability around one week after RV injection. Consistent with previous studies showing that SADΔG (EnvA) causes cell death in most infected neurons within weeks [5], our study showed that nearly all infected NG neurons died within 18 days. Tian *et al.* used an optogenetic tagging approach to record from dopamine neurons *in vivo*. They reported that RV-infected neurons show even stronger responses to reward cues in later days (days 10–15 post-infection) compared to earlier days (days 5–9) [10]. In present study, we found that cell viability decreased rapidly from day 7 to day 14 post-infection. This inconsistency is likely due to the differences in targeted neural circuits and recording methods. For instance, Ca^{2+} imaging ensured a clear identification of RV-infected neurons, whereas optogenetic tagging might also record from dopamine neurons not infected with RV that receive direct inputs from RV-infected presynaptic neurons.

The time windows of RV-based neural recording and manipulation have varied in previous studies: these can be short as three days and as long as two weeks depending on the species, application scenario, and targeted neural circuit [4, 10, 12]. Researchers may need to choose different optimal time windows for different scenarios. For instance, it is ideal to start neural recording and manipulation for *in vitro* experiments as soon as the RV-delivered gene is expressed, but behavioral tests may have to wait a few more days for animals to recover from surgery. Our data indicated that days 7–10 after RV injection was probably a feasible time window for applying SADΔG (EnvA)-based chemogenetics in feeding behavior studies. In summary, our systematic characterization of RV-induced neurotoxicity provides practical guidance for the use of the specific modified RV SADΔG (EnvA) in studies of neural circuit function.

Acknowledgements We thank members of the Neuroscience Pioneer Club for valuable discussions, and Yue Sun and Yanyan Fan (NIBS) for imaging assistance. This work was supported by the National Natural Science Foundation of China (31822026), the National Key R&D Program of China (2021ZD0203900), and a Shenzhen Science and Technology Innovation Commission grant (JCYJ20180507182505475).

Conflict of interest The authors declare that they have no conflict of interest.

References

1. Wickersham IR, Finke S, Conzelmann KK, Callaway EM. Retrograde neuronal tracing with a deletion-mutant rabies virus. Nat Methods 2007, 4: 47–49.
2. Luo F, Mu YL, Gao CC, Xiao Y, Zhou Q, Yang YQ. Whole-brain patterns of the presynaptic inputs and axonal projections of BDNF neurons in the paraventricular nucleus. Yi Chuan Xue Bao 2019, 46: 31–40.
3. Zhang SH, Lv F, Yuan Y, Fan CY, Li J, Sun WZ, *et al*. Whole-brain mapping of monosynaptic afferent inputs to cortical CRH neurons. Front Neurosci 2019, 13: 565.
4. Osakada F, Mori T, Cetin AH, Marshel JH, Virgen B, Callaway EM. New rabies virus variants for monitoring and manipulating activity and gene expression in defined neural circuits. Neuron 2011, 71: 617–631.
5. Wickersham IR, Lyon DC, Barnard RJ, Mori T, Finke S, Conzelmann KK, *et al*. Monosynaptic restriction of transsynaptic tracing from single, genetically targeted neurons. Neuron 2007, 53: 639–647.
6. Reardon TR, Murray AJ, Turi GF, Wirblich C, Croce KR, Schnell MJ, *et al*. Rabies virus CVS-N2c(ΔG) strain enhances retrograde synaptic transfer and neuronal viability. Neuron 2016, 89: 711–724.
7. Chatterjee S, Sullivan HA, MacLennan BJ, Xu R, Hou YY, Lavin TK, *et al*. Nontoxic, double-deletion-mutant rabies viral vectors for retrograde targeting of projection neurons. Nat Neurosci 2018, 21: 638–646.
8. Zhu XT, Lin KZ, Liu Q, Yue XP, Mi HJ, Huang XP, *et al*. Rabies virus pseudotyped with CVS-N2C glycoprotein as a powerful tool for retrograde neuronal network tracing. Neurosci Bull 2020, 36: 202–216.
9. Wertz A, Trenholm S, Yonehara K, Hillier D, Raics Z, Leinweber M, *et al*. PRESYNAPTIC NETWORKS. Single-cell-initiated monosynaptic tracing reveals layer-specific cortical network modules. Science 2015, 349: 70–74.
10. Tian J, Huang R, Cohen JY, Osakada F, Kobak D, Machens CK, *et al*. Distributed and mixed information in monosynaptic inputs to dopamine neurons. Neuron 2016, 91: 1374–1389.
11. Chen AX, Yan JJ, Zhang W, Wang L, Yu ZX, Ding XJ, *et al*. Specific hypothalamic neurons required for sensing conspecific male cues relevant to inter-male aggression. Neuron 2020, 108: 763-774.e6.
12. Tang YJ, Li L, Sun LQ, Yu JS, Hu Z, Lian KQ, *et al*. *In vivo* two-photon calcium imaging in dendrites of rabies virus-labeled V1 corticothalamic neurons. Neurosci Bull 2020, 36: 545–553.
13. Chen J, Cheng MX, Wang L, Zhang L, Xu D, Cao P, *et al*. A vagal-NTS neural pathway that stimulates feeding. Curr Biol 2020, 30: 3986-3998.e5.